

Deturbidization of vegetable oil refinery wastewater with extracted fish scale biomass via coagulation process; Non-linear kinetics studies

Abstract

Chito-protein was successfully synthesized from fish scale. The ability of a coagulant (chito-protein) prepared from fish scale (FSC) to carry out an effective removal of pollutants from food processing industry (vegetable oil industry wastewater, VOW) was evaluated at bench scale using a simulated jar test analysis. The coagulant was characterized via proximate analysis and instrumental analysis: Fourier transform infrared spectroscopy (FTIR) and scanning electron microscopy (SEM). The maximum kinetic parameters determined were recorded at K of $2 \times 10^{-5} \text{L/mg.min}$, 1g , $t_{1/2} = 50 \text{ min}$, $R^2 = 0.9245$ and pH of 2. Regression coefficient analysis (R^2) was used to ascertain the accuracy of the fit to the postulated kinetic model. However, it was concluded that the second order kinetic model described the reaction most adequately. Removal efficiency of turbidity (87.21%) was obtained at optimum contact time of 30 min, pH 2, coagulant dosage of 1.5g and temperature of 323K. Kinetic study showed that Pseudo first order and pseudo second order models were the best two models in describing the coag-adsorptive kinetics of the coagulant. Similarly, the predicted kinetic data were adjudged statistically significant using F- test and T-test.

Keywords: Wastewater, coagulation, fish scale, turbidity, kinetic model, non-linear

1.0 INTRODUCTION

Rapid industrialization has led to generation and unwholesome disposal of contaminated wastewater. Food processing (abattoir, vegetable oil etc.), paint, textile, pharmaceutical, cosmetics and plastic industries are among the industries that generates large volume of wastewater. Most of these wastewaters contain toxic substances (Okey-Onyesolu et al. (2016), high organic and inorganic dissolved solids, COD, BOD, and oil end which can be harmful if discharged untreated. The treatment of vegetable oil refinery wastewater (VOW) has been a major issue of environmental concern. Refining of crude vegetable oils generates large amounts of wastewater, which come from the degumming, de-acidification, deodorization and neutralization steps (Dkhissi et al., 2018). Its characteristics depend largely

37 on the type of oil processed, resulting in both high inorganic as well as organic pollutants
38 Moka (2015). Many processing techniques have been employed in the fight against pollution
39 in VOW, a wide variety of physicochemical processes has been proposed
40 (coagulation/flocculation, adsorption, photocatalysis, electrocoagulation, membrane
41 filtration) [Dkhissi et al., 2018]. Oil refinery wastewater treatment have gained increasing
42 importance, it can be treated either separately or in conjunction by chemical or biological
43 means. Biological treatment methods offer an easy and cost effective alternative to chemical
44 methods. Coagulation and flocculation as a unit process, in water and wastewater treatment
45 entails the use of metal salts (Al and Fe salts) (Xu et al, 2009). Also, the coagulation process
46 is one of the most effective methods of reducing/removing pollutants from wastewater. But
47 there are problems associated with chemical treatment which includes; the increased handling
48 costs and the production of chemical sludge that is difficult to treat (Dkhissi et al., 2018).
49 However, studies have discovered a number of drawbacks concerning the use of these
50 conventional coagulants. For example, Alzheimer's disease and other related problems are
51 associated with residual alum in treated water (Divakaran et al, 2001). To solve this problem
52 many types of natural reagents have been developed for removing pollutants from wastewater
53 chitosan (Roussy et al, 2005), tannins (Ozacar et al, 2002), aqueous extract of the seed of
54 moringa oleifera; extract of plantain peelings ash (Oladoja, 2008); and extracts of okra and
55 nirmali seed (Ani et al, 2010), they have advantages of being biodegradable and without risk
56 to public health, so a number of plant, animal or micro- organism sources are used in
57 wastewater treatment.

58 The present paper aims to valorise the fish scale chito-protein as a techno – economically and
59 eco-friendly coagulant for the treatment process of wastewater taken from vegetable oil
60 refining industry located at the south-east of Nigeria. The effects of the main experimental
61 conditions (initial solution pH, coagulant dosage, settling time and operating temperature) on
62 the coagulation treatment performance were studied. The coagulation process performance in
63 all cases was evaluated by means of the turbidity (TDSP).

64

65 **2.0 MATERIALS AND METHODS**

66 **2.1 Effluent collection and analysis**

67 A sample of vegetable oil refinery wastewater (VOW) was collected from an oil refinery
68 industry located in Onitsha, Anambra State, Nigeria and stored at room temperature. The
69 vegetable oil refinery effluent was preserved in dark plastic container to avoid photo-

70 reactions. The vegetable oil refinery wastewater sample was characterized before and after
71 treatment using standard methods (APHA, 1998).

72

73 **2.2 Processing of the coagulant from fish scale (FS)**

74 The fish scale (FS) was obtained from collected from Otuocha market in Anambra East,
75 Anambra state of Nigeria. The FS (Fig. 1) was washed thoroughly with water to remove
76 unwanted materials and sun dried for 14 days. It was crushed using a pestle and mortar to
77 reduce the size. The crushed sample was further air dried for five days to remove possible
78 remaining moisture. The ES sample was then transformed into powder using a grinding
79 machine and sieved with a laboratory sieve of known mesh size.

80 The powdered FS (Figure 2) was then processed into a coagulant (FSC), by adopting
81 modified Fernandez-Kim method described by (Ani et al., 2011). The product of
82 deproteinization of fish scale flour (FSF) was utilized instead of chitosan. For the
83 deprotenization, 1 L of 1M NaOH solution containing 100 g of FSF was stirred continuously
84 at 70 °C for 2h. The mixture was allowed to settle and cool. The mixture was separated
85 (using filter paper), the resulting solid sample has the potential of being processed further to
86 obtain chitosan however the extract from deprotenization process contains some percentage
87 of radical protein that will become a waste if not harnessed. The liquid extract was allowed to
88 settle for 30mins. The concentrated slurry settled at the bottom of the beaker was collected
89 (chito-protein), dried and stored for use.

90



91
92 Fig. 1 : Fish scale



93
94 Fig. 2: Fish scale flour

94 **2.3 Coagulation-Flocculation Experiment (Jar Test)**

95 The coagulation-flocculation experiments were performed using jar test apparatus. The
96 operating variables investigated were; initial effluent pH, chito-protein dosage, settling time
97 and operating temperature. The pH was controlled by adding either 1M HCl (acid) or 1M

98 NaOH (base). The VOW sample was mixed homogeneously before being fractionated into
 99 beakers containing 250ml of suspension each. The desired amount of chito-protein was added
 100 to each beaker containing the wastewater. Thereafter, the beakers were agitated at 250 rpm
 101 (fast mixing) for 2 minutes and 30 rpm (slow mixing) for 20 minutes. The effect of pH was
 102 studied at pH range (2 - 10) at varying chito-protein dosages in the range (0.5g – 2.5g) at
 103 different settling time and constant temperature. Thereafter, the effect of settling time was
 104 studied in the range (5 - 60 minutes) at varying coagulant dosages, optimum pH and constant
 105 temperature. The effect of temperature was then studied in the range (30 – 60°C) at varying
 106 settling time, optimum pH and coagulant dosage. The coagulation efficiency of the
 107 coagulants was investigated in terms of turbidity removal. Prior to the test, the sample was
 108 measured for turbidity, representing an initial turbidity. After settling at a specified time,
 109 samples were collected at 2 cm depth beneath the surface of the water for further turbidity
 110 measurement, representing the final turbidity. The residual turbidity (final turbidity) was
 111 converted to TDSP (mg/L), using a calibration curve at intervals of 5mins. The efficiency of
 112 turbidity removal was then evaluated using equation 1.

$$113 \quad \% \text{Removal} = \frac{T_0 - T}{T_0} \times 100 \quad (1)$$

114 Where; T_0 is the turbidity of raw effluent and T , the turbidity of effluent after treatment.

115 **2.4 Coagulation kinetic model description and theoretical principles**

116 The non-adsorptive kinetics of the process was modelled according to the description
 117 reported by (Menkiti et al., 2015; Ugonabo et al., 2012).

118 For a system operating at equilibrium phase with negligible impact of external Equations 2
 119 and 3 hold (Ugonabo et al., 2012):

$$120 \quad \mu_i = \bar{G}_i = \left[\frac{\partial G}{\partial n_i} \right]_{P,T,n} = \text{a constant}$$

121 (2)

$$122 \quad D' = K_B \frac{T}{B}$$

123 (3)

124 Where: D' is diffusion coefficient; B is friction factor; K_B is Boltzmann's constant; T is
 125 temperature; G is the total Gibbs free energy; n_i is the number of moles of component i ; μ_i is
 126 the chemical potential

127 for a case of mono dispersed, no break up and bi particle collision, floc formation depends
 128 on the rate of successful particles collision. For a particular floc size (Z) to be formed from
 129 particles of sizes i and j , this rate can be expressed as [Ani et al., 2011; Ugonabo et al., 2012]:

$$130 \quad \frac{dn_z}{dt} = \frac{1}{2} \sum_{i+j=z} \beta_{BR}(i, j) n_i n_j - \sum_{i=1}^{\infty} \beta_{BR}(i, k) n_i n_z$$

131 (4)

132 Where $\beta_{BR}(i, j)$ is Brownian collision factor for flocculation transport mechanism.

133 $n_i n_j$ is particle aggregation concentrations for particles of size i and j , respectively.

134 According to Ugonabo et al (2012):

$$135 \quad \beta_{BR} = \frac{8}{3} \varepsilon_p \frac{K_B T}{\eta}$$

136 (5)

137 And $K_R = 8\pi a D'$

138 (6)

139 Where: K_R is the Von smoluchowski rate constant for fast coagulation; a is particle radius;
 140 ε_p is the collision efficiency; η is the viscosity of the fluid medium.

141 Simplifying equations (6):

$$142 \quad K_R = \frac{4}{3} \frac{K_B T}{\eta}$$

143 (7)

144 Equations 4-5 could also be transformed to Eq. (7):

$$145 \quad K_m = \frac{1}{2} \beta_{BR}$$

146 (8)

147 Where: K_m is defined as Menkonu coagulation-flocculation rate constant accounting for
 148 Brownian coagulation-flocculation transport of destabilized particles at α^{th} order.

149 For Brownian coag-flocculation (Ugonabo et al, 2012):

$$150 \quad -\frac{dN_t}{dt} = K_m N_t^\alpha$$

151 (9)

152 N_t is the concentration of TDSP at time, t

153 Practically, it has been observed that: $1 \leq \alpha \leq 2$ (Ugonabo et al., 2012). Graphical
 154 representation of linear version of Eq. 9 at $\alpha = 1$ or 2 should produce a linear graph from
 155 which K_m could be determined from the slope of either Equation 10 or 11:

$$156 \quad \alpha = 1: \ln\left(\frac{1}{N}\right) = K_m t - \ln N_0$$

157 (10)

$$158 \quad \text{For } \alpha = 2: \frac{1}{N} = K_m t + \frac{1}{N_0}$$

159 (11)

160 Where N_0 is the initial N_t at time = 0

161 N is N_t at upper time limit > 0

162 Eq. (11) could be solved to obtain coagulation-flocculation period $\tau_{1/2}$

$$163 \quad \tau_{1/2} = \frac{1}{(0.5N_0 K_m)}$$

164 (12)

165 For Brownian controlled aggregation at $t \leq 30$ min, Eq. (12) could be solved exactly to
 166 generate Eq.13

$$\frac{N_{m(t)}}{N_0} = \frac{\left[\frac{t}{\tau_{1/2}} \right]^{m-1}}{\left[1 + \frac{t}{\tau_{1/2}} \right]^{m+1}}$$

167

168 (13)

169 **2.5 Particle Variations Behaviour as a Function of Time.**

170 The particle variations behavior plots of turbidity removal from vegetable oil refinery
 171 wastewater (VOW) was investigated.

172

173 **2.6 Adsorption kinetic model description**

174 The influence of adsorption on the coagulation process was investigated. The jar test data were
 175 subjected to series of adsorptive analysis. Three kinetic models were studied which includes: Pseudo
 176 first order, Pseudo second order and Elovich kinetic model. Table 1 presents the linear and
 177 corresponding non-linear model equations.

178 **Table 1: Linear and non-linear kinetic models**

| 179 | Kinetic equations | linear form | Non-linear | plot made | Eqn. No |
|-----|--|---|---|-----------------------|---------|
| 180 | Reference | | | | |
| 181 | Pseudo-first-order (Okoye et al., 2013) | $\log(q - q_t) = \log q - \left(\frac{K_1 t}{2.303}\right)$ | $q_t = q [1 - \exp(-k_1 t)]$ | $\log(q - q_t)$ vs. t | (14) |
| 182 | | | | | |
| 183 | Pseudo-second-order (15) (Okoye et al., 2013) | $t/q_t = \frac{1}{K^2 q_e^2} + \frac{t}{q_e}$ | $q_t = \frac{k_2 q_e^2 t}{1 + k_2 q_e t}$ | $\frac{t}{q_t}$ vs. t | |
| 184 | | | | | |
| 185 | Elovich (Okoye et al., 2013) | $qt = \left(\frac{1}{\beta}\right) \ln(\alpha\beta) + \left(\frac{1}{\beta}\right) \ln t$ | $q_t = \left(\frac{1}{\beta}\right) \ln (1 + \alpha_1 \beta t)$ | q_t vs. t | (16) |
| 186 | | | | | |
| 187 | | | | | |

188 **3.0 RESULTS AND DISCUSSION**

189 **3.1 Characterization of vegetable oil refinery wastewater (VOW) before and after**
 190 **coagulation**

191 The characterization result of the vegetable oil refinery wastewater before and after
 192 coagulation process is presented in Table 2. The vegetable oil refinery wastewater possessed
 193 high values of total suspended solids (TSS), biochemical oxygen demand (BOD), chemical

194 oxygen demand (COD), total suspended solids (TSS) and colour before treatment compared
 195 with the national regulatory standard for effluent discharge. Table 2 shows that the values of TSS,
 196 COD BOD among others recorded for the raw sample were well above national discharge standard,
 197 hence there is need for treatment before discharge. These values were reduced drastically after the
 198 coagulation treatment (see table 1), affirming the effectiveness of the coagulation in
 199 achieving organic load reduction (Obiora-Okafo and Onukwuli, 2013).

200 Table 2: Characterization result of VOW before and after coagulation using FSC

| Parameter | Before Coagulation | After Coagulation |
|----------------------|--------------------|-------------------|
| Turbidity(NTU) | 280 | 14 |
| TSS (mg/l) | 389.2 | 24 |
| COD (mg/l) | 933 | 65 |
| BOD (mg/l) | 634 | 37 |
| pH(-) | 6.9 | 7.3 |
| Colour (mg/l) | 630.6 | 88 |
| TS (mg/l) | 688 | 58 |
| TDS (mg/l) | 298.8 | 34 |
| Total hardness(mg/l) | 43.8 | 19 |
| Sulphate (mg/l) | 18 | 2.4 |
| Iron (mg/l) | 0.632 | 0.13 |
| Potassium (mg/l) | 2.87 | 0.6 |
| Magnesium (mg/l) | 19.49 | 4.71 |
| Lead (mg/l) | 0.10 | - |

201

202 Note: NTU-nephelometric turbidity unit, TDS-total dissolved solids, TSS-total suspended
 203 solids, COD-chemical oxygen demand and BOD -biochemical oxygen demand

204 3.2 Characterization result

205 3.2.1 Physiochemical characterization

206 The bio-coagulant extracted from the fish scale flour was subjected to proximate analysis. The
 207 properties measured are percentage Moisture, Crude protein, Ash content, crude fibre,
 208 Carbohydrates and Lipid content. The characteristics of FSC presented in Table 3 show that

209 it has a reasonably high content of protein (19.11%). This is an indication of its likely good
 210 performance as a coagulant for wastewater treatment.

211 **Table 3: Proximate analysis of FSC**

| | |
|-------------------|-------|
| Moisture (%) | 7.48 |
| Crude protein (%) | 19.11 |
| Ash content (%) | 25.08 |
| Crude fibre (%) | 3.05 |
| Lipid content (%) | 2.98 |
| Carbohydrates (%) | 42.3 |

212

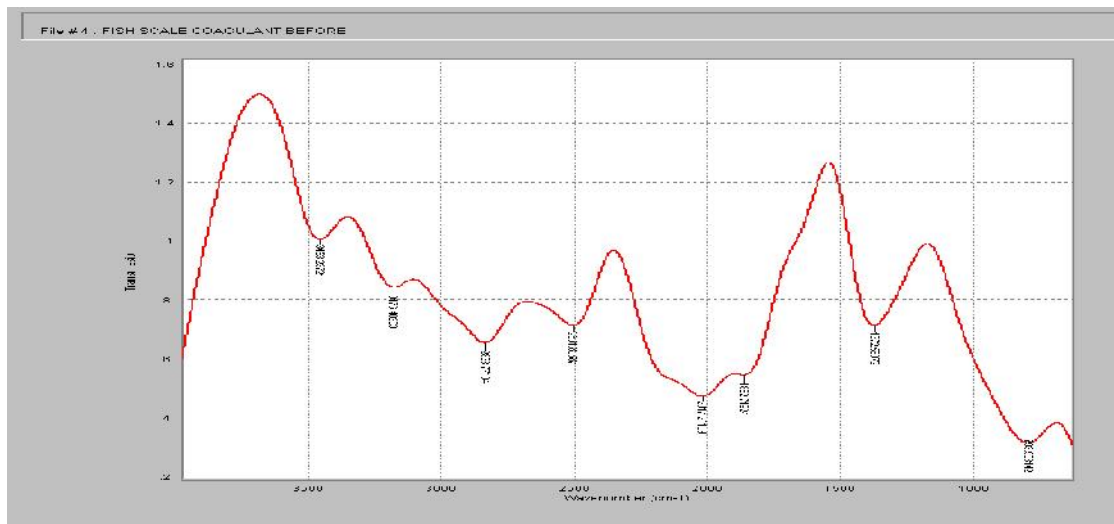
213 3.2.2 FTIR analysis

214

215 The FTIR spectra of the raw and extracted polymer (chito-protein) derived from fish scale are
 216 shown in figures 3 and 4 respectively. The results were analyzed based on the standard peaks
 217 as presented by Silverstein et al. (1981) for various functional groups. The comparison of the
 218 spectra results of the coagulant precursors and the synthesized coagulants indicates an
 219 obvious shift, disappearance and detection of new wave numbers. This observation could
 220 have existed as a direct consequence of the chemical reaction process involved in the
 221 coagulant synthesis and further elucidates the existence of improved/modified chemical
 222 species on the coagulants. This chemical modification could ultimately result in an improved
 223 coagulation performance by the respective coagulants. Table 4 provides detailed information
 224 on raw and extracted coagulant with respect to the various peaks that shifted, vanished or
 225 appeared. The wave number shifts in the spectra image of the coagulant are observed to range
 226 between $\pm 2\text{cm}^{-1}$ to as high as $\pm 147\text{ cm}^{-1}$ (see Table 4). Another important observation made
 227 with respect to Table 4 is that there were negligible wave number differences between FSF
 228 and FSC when compared to the other materials. This finding suggests a limited reactivity of
 229 the respective functional groups in FSF during the synthesis of FSC.

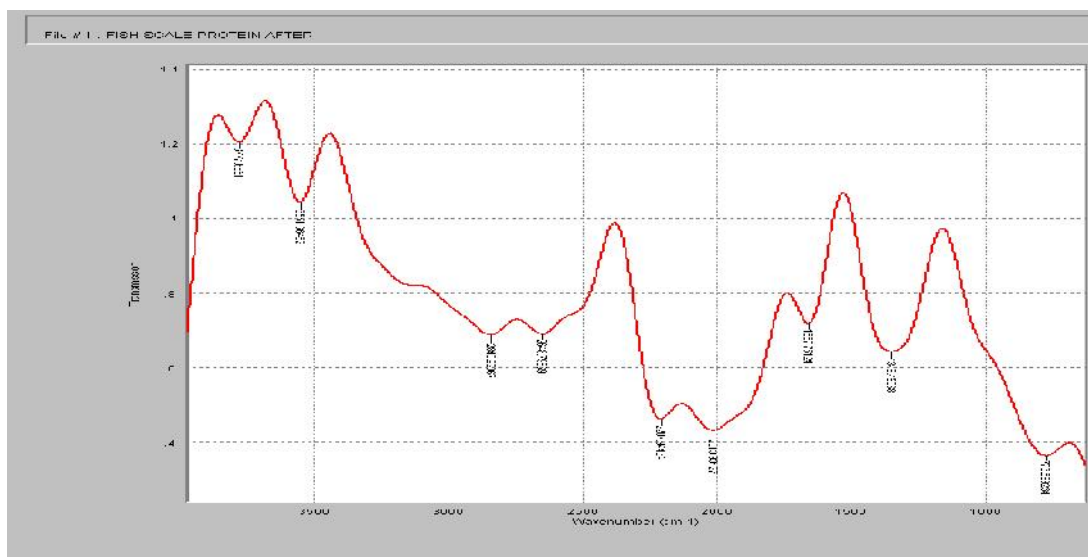
230 Vibrational peaks observed from the analysis were made are presented in table 4 and figures
 231 3 and 4. Usually the absorption peaks observed below 500 cm^{-1} are not applicable for the
 232 characterization of fish scale (Fernandez-Kim, 2004). At the higher wave number end of the
 233 spectra, the C – H stretching region provides important information about the coagulants'
 234 chemical composition. The distinct stretching band at wave numbers greater than 3000 cm^{-1}
 235 suggests the existence of aromatic ring groups in the coagulant structure (Günter and David,
 236 2014). The peak at 793.9931cm^{-1} can be attributed C-H bending vibration while that at

237 1348.451 cm^{-1} can be assigned to SO_2 asymmetric band. Additionally, the absorption peak at
 238 3453.237 cm^{-1} which is within the range of 3200 and 3500 cm^{-1} which were characteristic of
 239 N-H stretching of amides (Stuart, 2004).



240

241 Figure 3: FTIR spectrum analysis of FSF sample



242

243 Figure 4: FTIR spectrum analysis of FSC sample

244 Table 4: FTIR table for vibrational peaks of fish scale (FSF and FSC)

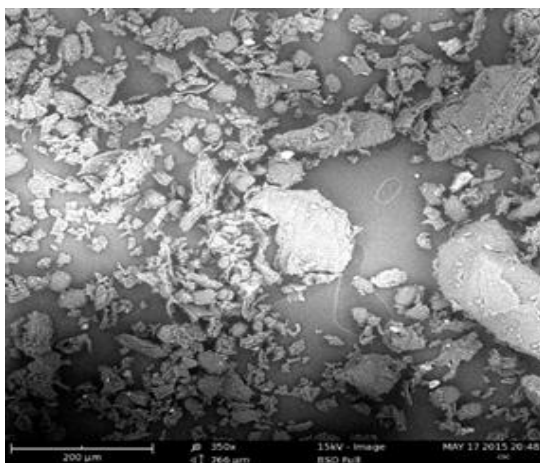
| Peak (cm^{-1}) | | | |
|---------------------------|----------|-------------|--------------------------------|
| FSF | FSC | Differences | Assignment |
| 793.9931 | 773.6992 | 20.29 | Out – of – plane C – H bending |
| 1372.581 | 1348.451 | 24.13 | SO_2 asymmetric band |

| | | | |
|----------|----------|--------|---------------------------------------|
| x | 1657.751 | x | NO ₂ asymmetric stretching |
| 1862.719 | x | | C = O stretching |
| 2017.211 | 2013.944 | 3.28 | Metal carbonyl C = O |
| x | 2207.94 | x | |
| 2501.807 | 2648.799 | 146.99 | Phosphoric acid and Ester O – H |
| 2833.771 | 2840.921 | 7.15 | C – H stretching of aldehyde |
| 3176.483 | x | x | O – H stretching of carboxylic acid |
| 3453.237 | x | x | N – H stretching |
| x | 3551.365 | x | Si – OH stretching |

245

246 3.2.3 Scanning electron microscopy (SEM) characterization of FSC and FSC

247 The SEM technique, a powerful tool for analysing the surface morphological make-up of the
 248 polymeric coagulants was employed. SEM image was used to elucidate the surface texture
 249 and morphology of the synthesized coagulant. The result of the SEM studies for the raw (fish
 250 scale flour) extracted (FBC) samples were presented in plates 1 and 2.



251

252 Plate 1: SEM micrograph of FSF

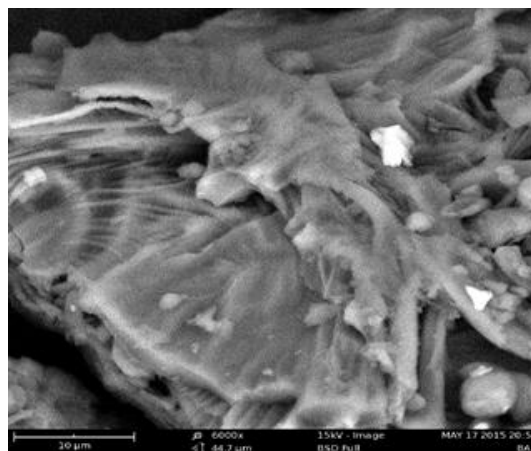


Plate 2: SEM Micrograph of FSC

253 Plates 1 and 2, show the SEM micrographs of fish scale flour and fish scale chito-protein
 254 respectively. Plate1 was mainly characterized by smooth surface with seemingly compact
 255 structures. It also exhibits the appearance of tiny homogenous pores. While, Plate 2 shows the
 256 existence of irregular granular structure on the coagulant morphology. The appearance of
 257 irregular platelets on plate 2 shows that fish scale coagulant (FSC) has rough edges which

258 may be attributed to high brittle property of the coagulant, (Obiora-Okafo et al., 2014). Also,
 259 according to Obiora-Okafo (2011), irregular granular structures are desirable characteristics
 260 of any coagulant with regards to adsorbing and bridging of colloidal particles and further
 261 enhancing the sedimentation of flocs. Multiple pores can also be visualized on plate 2; these
 262 pores are available sites for particles adsorption.

263 3.5 Factor Sensitivity studies

264

265 Various factors influence the coagulation performance of any given coagulant. The influences
 266 of the variation of some of these factors are highlighted in section 3.5.1 to 3.5.3;

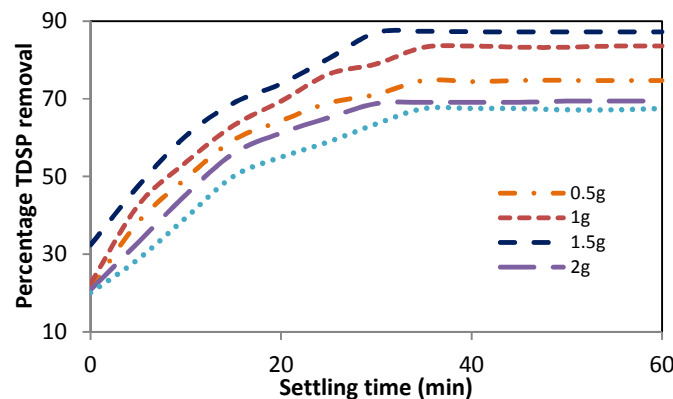
267

268 3.5.1 Effect of FSC dosages and setting time on TDSP removal efficiency

269

270 The effect of coagulant dosage (FSC) at different settling time on TDSP removal efficiency
 271 from vegetable oil refinery wastewater was analysed at initial pH of the wastewater. Fig. 5
 272 shows the plots of removal efficiency of TDSP against settling time at varying dosages. The
 273 result of the turbidity removal with respect to FSC dose is presented in Fig. 5. The dosage
 274 studied varied from 0.5-2.5g. The graph (Fig.5) indicates that the removal TDSP increased
 275 with increase in the coagulant dosage. The percentage turbidity removal recorded for
 276 coagulant dose of 1g was 74.7% at 30min. Similarly, at a coagulant dose of 1.5g over the
 277 same time, the percentage TDSP removal was 84.0%. The increase in the TDSP removal with
 278 an increase in FSC dose could be attributed to the availability of large content of protein
 279 created by more quantity of coagulant deposited to the wastewater which aid to fast
 280 coagulation process.

281



282 Fig 5: Effect of coagulant dosage

283

284

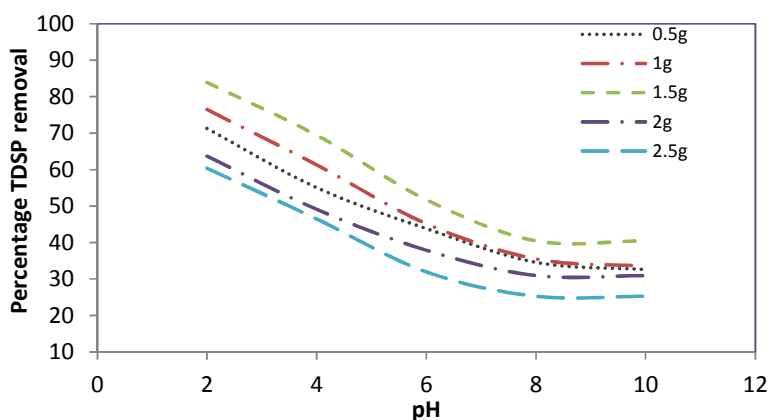
285

286

287 3.5.2 Effect of pH on turbidity removal efficiency

288

289 The effect of pH was studied at the varying coagulant dosage, temperature of 30°C, and time
 290 of 60min as shown in Fig.6. The pH of the wastewater was varied from 2-10 using H₂SO₄
 291 and NaOH. The result is shown in Fig. 6 for TDSP. An optimum TDSP removal efficiency of
 292 84% was obtained at pH of 2 with 1.5g optimum coagulant dose. This shows that the
 293 treatment process performs better when the solution is in acidic medium. In addition, after the
 294 pH of 2, the removal efficiency of the particles decreased continuously till the minimum
 295 value was attained, this trend can be attributed to decrease in solubility of coagulant with
 296 increase in pH. Hence, it was evident that FSC may not be very effective in alkaline solution.
 297 Similar works were reported by Devi et al (2012).



298

299 Fig 6: Effect of pH

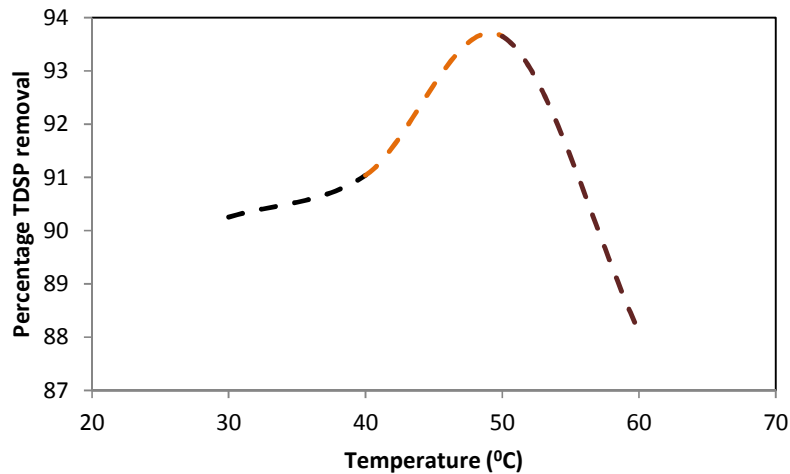
300

301 3.5.3 Effect of temperature on TDSP removal efficiency

302

303 The effect of temperature on the coagulation efficiency was investigated at the best pH and
 304 best coagulant dose while varying the temperature between 30 – 60°C. From the efficiency
 305 analysis, it was observed that the coagulation efficiency varies directly with temperature to
 306 the maximum (Fig. 7) and decreased thereafter. The ascending part can be attributed to
 307 particle excitement; hence at this stage more flocs are formed. After the maximum stage
 308 (50°C), decrease in particle removal with temperature was observed at temperature of 60°C.

309 This could be as a result of denaturation of the coagulant particles which may cause slight
 310 inhibition of the process. Similar result was obtained by Babayemi et al. (2013)
 311

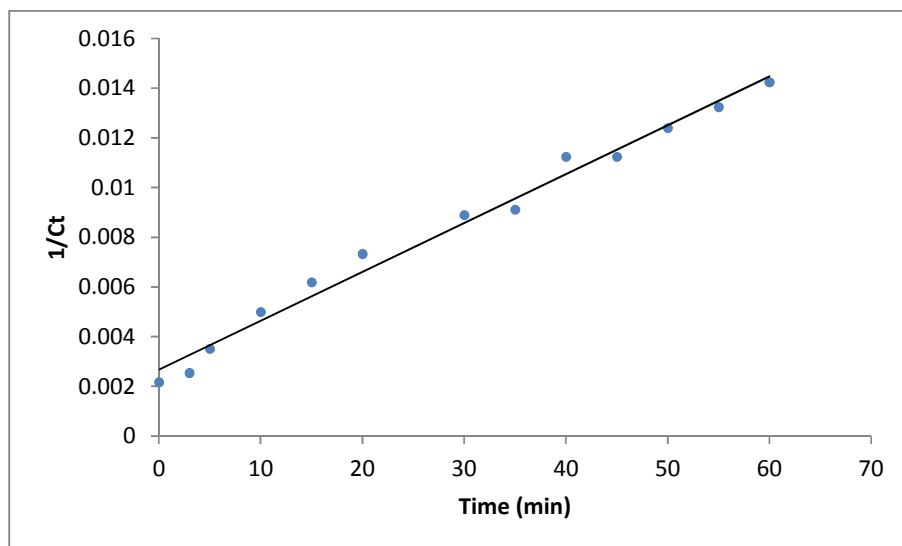


312

313 **Fig. 7: Effect of temperature on turbidity (%) removal**

314 3.6 Coagulation Kinetics

315 The kinetics of TDSP removal was evaluated to study the effect of time on the particle
 316 movement from the bulk of the effluent sample to the surface of the coagulant after charge
 317 neutralization and destabilization, the kinetic plot ($\frac{1}{C_t}$ vs t) that described the rate of particle
 318 transport is presented in Fig. 8, while the calculated parameters are presented in table 5.



319

320

321 Fig. 8: Plot of $1/Ct$ against settling time for

322

323 Brownian transport of destabilized particles (K_m) for the rate constant was evaluated from
 324 the slope of the kinetic plot of $1/Ct$ against t (Fig 8), while the Von smolushoski's
 325 coagulation constant (K_R) accounts for the rate of rapid coagulation was determined based on
 326 equation 11. For perikinetic coagulation with a constant order of 2, the difference between
 327 K_m and K_R accounts for the rate of particle flocculation (K_f). The K_m was obtained as $2E-$
 328 $05g/min$ while K_m was obtained as $4.86E-21$. The rate of particle flocculation was
 329 $0.00002g/min$. The number of effective collision was estimated as a function of particle
 330 collision efficiency (ϵ_p). Higher value of (ϵ_p) obtained in the system suggests that more
 331 collision leads to floc formation. Table 5 shows the parameters obtained. From table 5, it can
 332 be observed that $K_m \gg K_R$ which shows that K_R is quite negligible relative to K_m . The result
 333 suggests that the entire process is greatly influenced by the rate of floc formation than the
 334 actual rate of coagulation.

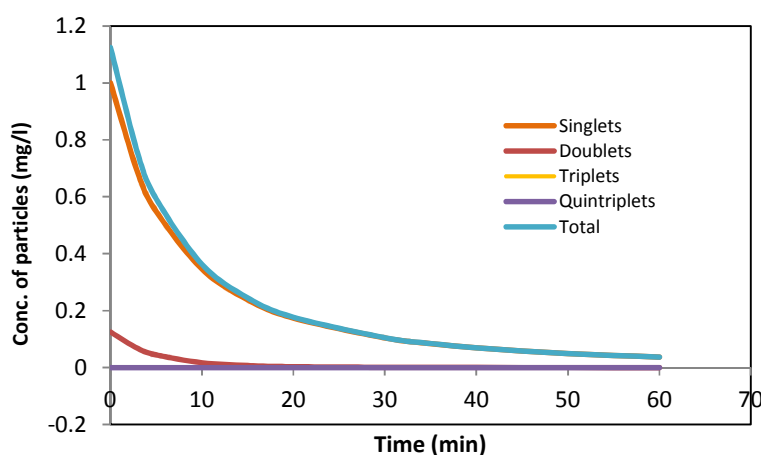
Table 5: coagulation kinetic parameters

| Parameters | |
|-------------------|-------------|
| $K_m(g.min)$ | 2.00E-05 |
| R^2 | 0.9245 |
| $\beta Br(g.min)$ | 0.00004 |
| $\tau_{1/2}(min)$ | 50.00 |
| r | 1.11E-05 |
| ϵ_p | 4.12E+15 |
| K_R | 4.86E-21 |
| D' | 1.74E-17 |
| B | 0.000239917 |
| α | 2.0000 |

335 3.7 Particle distribution

336 The total number of turbidity concentration, N_t and the concentration of the species N_i both
 337 decrease monotonically with increasing time. From the plot, the concentrations of $N_2(t)$, N_3
 338 (t) and $N_4(t)$ pass through a maximum (Santhanam et al., 2014). This is because they are not

339 present at $t = 0$ and $N_0 = 0$. The number of singlet (N_1) can be seen to decrease more rapidly
 340 than the total number of particles N_i . This happens as a result of increasing number of
 341 particles concentration on aggregate formation with time (Menkiti and Ejimofor, 2016). Here,
 342 the total number of particles decreases according to a bimolecular reaction. From the plot, it
 343 can be observe that the lower the value of K , the higher the coagulation time T_{ag} with respect
 344 to its N_0 and the more the effect of high period of particle distribution (Obiora et al. 2014).
 345 At low K the rate process is very slow which gives rise to more time for the coagulation-
 346 flocculation process. Fig. 9 shows the effect of high period of particle distribution. Here, the
 347 decrease of singlets from initial particle concentration and increase in doublets, triplets and
 348 quadruplets from zero concentration occur. The sum of all the distribution particles from
 349 singlets, doublets, triplets and quadruplets display the overall effects of high period on the
 350 reactor. This suggests low rate of particle aggregation and poor particle removal efficiency
 351 (Menkiti and Ejimofor, 2016).



352

353

Fig.9: Particle distribution plot for TDSP removal

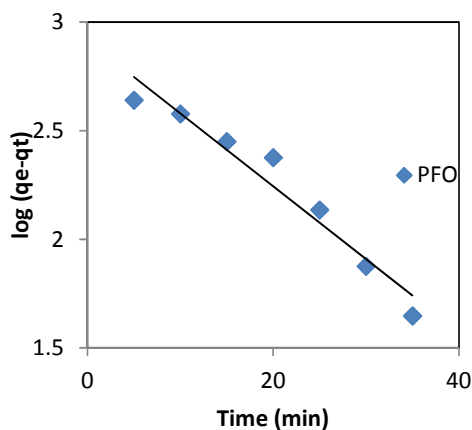
354

355

3.6 Coag-adsorptive kinetic studies

356 Coagulation is known to be a multi-component process where four mechanisms can be
 357 identified. The mechanisms include; double layer compression, adsorption and charge
 358 neutralization, sweep flocculation and adsorption and inter-particle bridging. These
 359 mechanisms are grouped into adsorptive and non-adsorptive components. To describe the
 360 adsorptive component of the process, adsorption kinetic models were used to model the
 361 coagulation kinetic data obtained during the experimental studies. For this present studies,
 362 three (3) kinetic models were considered which includes: PFO, PSO and Elovich kinetic
 363 models. Figs. 10, 11 and 12 show the linear plots of PFO, PSO and Elovich kinetic models.
 364 While Fig. 13 shows the comparative relationship between the nonlinear model data and the

365 experimental data. Also, table 6 shows the calculated model parameters, their statistical T-
 366 Test, F-test, STD and Chi test estimated can also be identified in the same table 6.



367

368 Fig. 10: Linear plot of PFO kinetic model

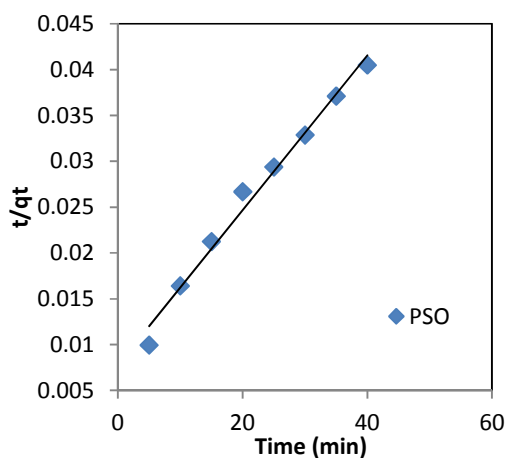
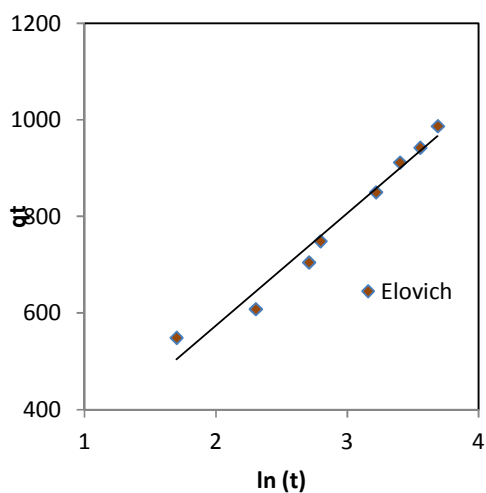


Fig. 11: Linear plot of PSO kinetic model



369

370 Fig. 12: Linear plot of Elovich kinetic model
 371 kinetics

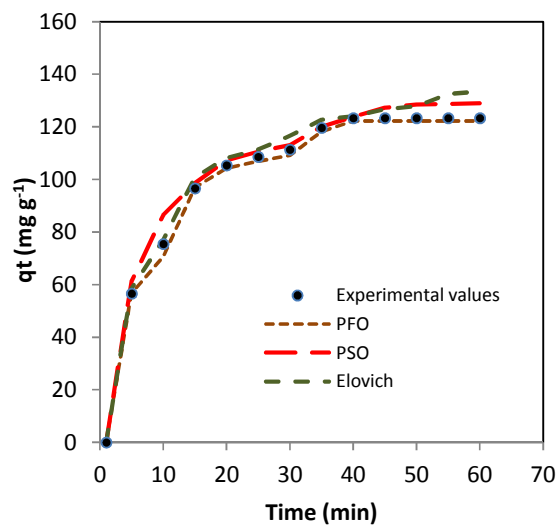


Fig. 13 kinetic modeling of the coag-adsorptive

Table 6: kinetic parameters for linear and non-linear kinetic models

| PSO | | PFO | | Elovich | |
|--------------------|----------|--------------------|----------|-----------------------|----------|
| K (linear) | 0.000846 | K (linear) | 0.01624 | β (linear) | 0.046268 |
| R^2 (linear) | 0.9974 | R^2 (linear) | 0.9873 | α (linear) | 24.89146 |
| K(non-linear) | 0.00283 | K (non-linear) | 0.01624 | R^2 (linear) | 0.9607 |
| q_e (linear) | 129.9479 | q_e (linear) | 107.9941 | β (non-linear) | 0.163284 |
| q_e (non-linear) | 129.7413 | q_e (non-linear) | 109.0498 | α (non-linear) | 44.72479 |
| R^2 non-linear | 0.9945 | R^2 non-linear | 0.9909 | R^2 (non-linear) | 0.9738 |
| T-test | 0.036036 | T-test | 0.000715 | T-test | 0.000232 |
| F-test | 0.712126 | F-test | 0.886854 | F-test | 0.835209 |

| | | | | | |
|--------------|----------|--------------|----------|--------------|----------|
| Chi test | 0.99906 | Chi test | 0.994527 | Chi test | 0.996882 |
| STD | 20.08663 | STD | 20.8065 | STD | 21.98474 |
| Δq_e | 0.206587 | Δq_e | 1.0557 | Δq_e | 10.05778 |

372 The Pseudo first order and pseudo second order models assume that the adsorptive
 373 component of coagulation is a pseudo chemicals reaction, while the kinetic data follow
 374 Elovich model if the adsorption is chemical in nature. In this present study, it was observed
 375 that the coefficient of correlation for models considered were above 0.9 for both linear and
 376 non-linear studies. Hence the difference between $q_{(e \text{ exp})}$ and $q_{(e \text{ cal})}$ (Δq_e) was used as the
 377 basis of model comparison. Where $q_{(e \text{ exp})}$ is the quantity adsorbed at equilibrium time, while
 378 $q_{(e \text{ cal})}$ is model generated data. From table 6, the models with $(\Delta q_e) \geq 2$ were considered as
 379 having poor description of the experimental kinetic data. Hence, pseudo second order and
 380 pseudo first order kinetic models with $(\Delta q_e) < 2$ were considered.

381 4.0 CONCLUSION

382 Fish scale has been identified as a potential source of coagulation agent for the removal of
 383 turbidity from vegetable oil industry effluent. Some of the parameters that control bio-
 384 coagulation were found to include coagulation pH, coagulant dosage, and coagulation
 385 temperature. It was observed that the percentage turbidity removal increased with increase of
 386 the settling time. The optimum contact time, pH and temperature were 30 min, 2 and 323K
 387 respectively. By applying 3 different linear and nonlinear kinetic models to evaluate the
 388 optimum parameter sets; Pseudo first order and Pseudo second order models were found to be
 389 the best two most suited models (judging by the maximum correlation coefficient, R^2 and
 390 least Δq_e value. Using statistical tools (F-test and student's t-test) the predicted kinetic data
 391 were adured statistically significant. The FT-IR spectrum confirmed the chemical structures
 392 of both the fish scale flour and their corresponding coagulant (FSC) with the functional ester
 393 groups present. The kinetics of the coagulation/flocculation reaction presented showed that
 394 the reaction followed second order kinetic model. Since, fish scale performed very well in the
 395 coagulation studies performed, there is therefore great possibility of replacing chemical
 396 coagulants with less hazardous and efficient bio-coagulants.

397

398 NOMENCLATURES

399 VOW: Vegetable oil refinery wastewater

400 FSF: Fish scale flour

401 FSC: Fish scale coagulant

402 TDSP: Total suspended and dissolved particles

403 FTIR: Fourier transforms infrared

404 T_o : Turbidity of raw effluent

405 T: Turbidity of effluent after treatment

406 TSS: Total suspended solid

407 TS: Total solid

408 COD: Chemical oxygen demand

409 BOD: Biochemical oxygen demand

410

411 REFERENCES

412

413 Ani J.U, Menkiti,M.C and Onukwuli,O.D (2010). Coagulation and Flocculation behaviour of
414 snail shell coagulant in fibre-cement plant effluent, J.Eng.Appl.Sci.67, 2.

415 APHA (1998). Standard Methods for Water and Waste Water Examination. 16th Edition,
416 American Public Health Association (APHA), Washington DC, USA

417 Babayemi K.A., Onukwuli O.D & Okewale A.O. (2013). Coag-Flocculation of Phosphorus
418 Containing Waste Water Using Afzella-Africana Biomass. *International Journal of*
419 *Applied Science and Technology* Vol. 3 No. 6, pp 43-50.

420 Devi G., Shinoon A.H. and Sekhar G.C., (2012). Treatment of vegetable oil mill effluent
421 using crab shell chitosan as adsorbent. *International journal of Environmental*
422 *Science and Technology* 9(4) DOI:10.1007/s13762-012-0100-4

423 Divakaran R. and Pillai V.N.S. (2001). Flocculation of kaolinite suspension in water by
424 chitosan, *Water Res.* 35, 3904-3908.

425 Dkhissi O., El Hakmaoui A., Souabi S., Chatoui M., Jada A., Akssira, M. (2018). Treatment
426 of vegetable oil refinery wastewater by coagulation-flocculation process using the
427 cactus as a bio-flocculant. *Journal of Materials and Environmental Sciences*, 9 (1),
428 18-25.

429 Fernandez-Kim S. (2004), Physiochemical and Functional properties of crawfish chitosan as
430 affected by different processing protocols, M.Sc Thesis,Louisiana State University
431 and Agricultural and MechanicalCollege,USA.

- 432 Günter, G and David S.M (2014) Handbook of spectroscopy, 2nd edn. John Wiley & Sons,
433 Hoboken. <https://doi.org/10.1002/9783527654703>.
- 434 Menkiti M.C, Ganesan S, Ugonabo V. I, ' Menkiti N. U, Onukwuli O.D., (2015), Factorial
435 optimization and kinetic studies of coagulation-flocculation of brewery effluent by
436 crab shell coagulant;Journal of the Chinese Advanced Materials Society.
- 437 Menkiti, M. C., Ejimofor, M. I.,(2016). Turbidmetric Approach on the study of Adsorptive
438 component of paint effluent coagulation using snail shell extract, Arabian journal for
439 science and Engineering 41,7, 2527-2543.
- 440 Moka, K.B (2015). Technical Report on SIWES undertaken at a vegetable oil Industry.
441 Nnamdi Azikiwe University, Nigeria.
- 442 Obiora-Okafo, I. (2011). Treatment of brewery wastewater using coagulation-flocculation
443 and adsorption techniques. Unpublished Masters' Thesis, Department of Chemical
444 Engineering, Nnamdi Azikiwe University Awka, Nigeria. 65.
- 445 Obiora-Okafo, I.A., and Onukwuli, O.D. (2013). Utilization of sawdust (*Gossweilerodendron*
446 *balsamiferum*) as an adsorbent for the removal of total dissolved solid particles from
447 wastewater. International Journal of Multidisciplinary Sciences and Engineering,
448 4(4): 45 – 53.
- 449 Obiora-Okafo, I.A., Menkiti, M.C., and Onukwuli, O.D. (2014). Utilization of response
450 surface methodology and factor design in micro organic particles removal from
451 brewery wastewater by coagulation / flocculation technique. Inter. J. of Appl. Sci.
452 and Maths., 1(1): 15 – 21.
- 453 Okey-Onyesolu,C.F. Onukwuli, O. D. Okoye, C. C. and Nwokedi I. C. (2016). Removal of
454 heavy metal pb(II) ions from aqueous solution using pentaclethra macrophylla and
455 tetracarpidium conophorum seed shells based activated carbons: equilibrium,
456 kinetics and thermodynemics studies. British Journal of Applied science &
457 Technology,16(6): 1-20.
- 458 Okoye, C. C, Onukwuli, O. D, Okey-Onyesolu, C. F and Nwokedi, I. C (2013): Adsorptive
459 Removal of Erythrosin B Dye onto *Terminalia Catappa* Endocarp Prepared
460 Activated Carbon: Kinetics, Isotherm and Thermodynamics Studies.

- 461 Oladoja N.A. and Aliu Y.D. (2008); Evaluation of plantain peelings ash extract as coagulant
462 aid in the coagulation of colloidal particles in low pH aqua system, Water Quality
463 Research Journal, Canada.
- 464 Ozacar, M.and Sengil,I.A(2002). Effectiveness of tannins obtained from velonia as a
465 coagulant aid for dewatering of sludge. Water res.34(4);1407-1412.
- 466 Roussy J., Chastellan P., Vooren M. and Guibal E. (2005). Treatment of ink-containing waste
467 water by coagulation/flocculation using biopolymers, Water SA 31 (3), pp 369-376.
- 468 Santhanam Needhidasan, Melvin Samuel, and Ramalingam Chidambaram (2014).Electronic
469 waste – an emerging threat to the environment of urban India. J.Environ Health Sci
470 Eng. doi: 10.1186/2052-336X-12-36.
- 471 Silverstein, R.M.; Bassler, G.C.; and Morrill, T.C. (1981). Spectrometric Identification of
472 Organic Compounds. 4th ed. New York: John Wiley and Sons. New York, USA.
- 473 Stuart, B (2004) Infrared spectroscopy: fundamentals and applications. John Wiley & Sons,
474 Hoboken.
- 475 Ugonabo, V.I., Menkiti, M.C., Onukwuli, D.O. (2012). Effect of coag-flocculation kinetics
476 on telfairia occidentalis seed coagulant (TOC) in pharmaceutical wastewater.
477 International Journal of Multidisciplinary Sciences and Engineering, 3(9), 22-33.
- 478 Xu C.R.,Yan Z.C. and Wang Y.C.(2009); Recycle of alum recovered from water treatment
479 studies in chemically enhanced water treatment; Journal of hazardous materials 161
480 pp 663-669.